Free Radical Formation and Characterization of Nitroanisole Isomer Reduction in Different Media

Luis J. Núñez-Vergara,[a,z] S. Bollo,[a] A. M. Atria,[b] J. Carbajo,[b] S. Gunckel,[a] and J. A. Squella[a]

[a]*Laboratory of Bioelectrochemistry, Faculty of Chemical and Pharmaceutical Sciences,*
[b]*University of Chile, Santiago, Chile*

A comprehensive study of the electrochemical characteristics of 2-, 3-, and 4-nitroanisole isomers in three different electrolytic media has been carried out. Furthermore, kinetic characterization of the one-electron reduction product from these isomers in these media is also reported. Also, free radicals were characterized in aprotic media by electron paramagnetic resonance through their corresponding hyperfine splitting constants. In protic media (30% ethanol/0.1 M Britton-Robinson buffer pH 2-12) 2-, and 3-nitroanisole isomers gave an irreversible well-defined peak over the entire pH range on Hg in a reaction involving four electrons to give the hydroxylamine derivative. However, in the case of 4-nitroanisole the kinetic characterization of the corresponding nitro radical anion was successfully achieved in this medium at pH 10.5, exhibiting a k_{2disp} value of 19,000 $(Ms)^{-1}$. In this medium the ease of reduction at pH 7 was 2-nitroanisole (2-NA) > 3-nitroanisole (3-NA) > 4-nitroanisole (4-NA). In mixed aqueous-organic media [0.015 M aqueous citrate dimethylformamide (DMF): 60:40, 0.3 M KCl, and 0.1 M tetrabutylammonium iodide (TBAI) at pH ⩾ 10.5 the isolation of the couple by cyclic voltammetry and the electrochemical characterization of the nitro radical anion corresponding to the three compounds were achieved. Calculated disproportionation second-order rate constants, k_{2disp}, had an average value of 10,900 ± 930 $(M\ s)^{-1}$, 2400 ± 400 $(M\ s)^{-1}$, and 5000 ± 600 $(M\ s)^{-1}$ for 2-NA, 3-NA, and 4-NA, respectively. Also, the reactivity of the radicals toward glutathione was quantitatively assessed through the calculation of the respective apparent interaction rate constants. In aprotic media (0.1 M TBAI in DMF) the nitro radical anions were more stable than in the mixed media, with the following second-order decay rate constant, k_{2dim}, values: 1100 ± 100 $(M\ s)^{-1}$, 1600 ± 150 $(M\ s)^{-1}$, and 650 ± 70 $(M\ s)^{-1}$ for 2-NA, 3-NA, and 4-NA, respectively.

Nitroaromatic compounds are released into the biosphere almost exclusively from anthropogenic sources. Some compounds are produced by incomplete combustion of fossil fuels; others are used as synthetic intermediates, dyes, pesticides, drugs, and explosives. Recent research has revealed a number of microbial systems capable of transforming or biodegrading nitroaromatic compounds. Anaerobic bacteria can reduce the nitro group via nitroso and hydroxylamino intermediates to the corresponding amines.[1,2]

Now it is widely accepted that biological (therapeutic and toxic) properties of nitrocompounds reside in the electrochemical characteristics of the nitro group, *i.e.*, ease of nitro-reduction, stability of radicals and reactivity of redox intermediates with cellular components' the most relevant being nitro radical anion formation. Therefore, the reduction properties of the nitro group have received considerable attention, mainly using pulse radiolysis,[3] electron spin resonance (ESR) spectroscopy,[4,5] and also electrochemical techniques.[6-10] Specifically, concerning biological studies on nitroanisole isomers, recently[11] it has been demonstrated *in vitro* that 2-nitroanisole participates in both the initiation and the promotion phases of carcinogenesis. Furthermore, DNA single-strand breaks in fire fighters accidentally exposed to 2-nitroanisole and other chemicals liberated into the environment have also been reported.[12] In both cases, the formation of active oxygen species was found, probably as a consequence of biotransformation reactions involving 2-nitroanisole, either reduction or oxidation reactions. Literature about of the electrochemistry of nitroanisole isomers is rather restricted. However, Vianello *et al.*[13,14] have previously carried out a comparative study of nitrophenols and nitroanisole isomers in aprotic media.

Considering that generation of radical species is relevant for biological activity and that nitroanisole isomers constitute a very interesting chemical prototype of nitrocompounds with pharmacological and toxicological properties, a comprehensive study of their electrochemical characteristics in different electrolytic media has been carried out. Moreover, in this paper focus has been put on the kinetic characterization of the one-electron reduction product of the nitroanisole isomers in the different electrolytic media. Also, we report the reactivity of radicals in mixed media with glutathione and their electron paramagnetic resonance (EPR) characterization in aprotic media.

Experimental

Drugs and reagents.—2-nitroanisole (2-NA), 3-nitroanisole (3-NA), 4-nitroanisole (4-NA), dimethylformamide (DMF, spectroscopic grade), nitrobenzene, tetrabutylammonium iodide (TBAI), and tetrabutylammonium hydroxide, were purchased from Merck Laboratories (Santiago, Chile).

Polarography.—Differential pulse (DPP) and Tast polarography experiments were carried out with an Inelecsa® assembly PDC 1212 containing generator/potentiostat with an A/D converter interface attached to a 12-bit microprocessor and suitable software for totally automatic control of the experiments and data acquisition. A Gateway microcomputer was used for data control, acquisition, and treatment.

Operating conditions: pulse amplitude 60 mV; potential scan 5 mV/s; drop time 1 s; voltage range 0 to −2000 mV; current range 1.25-5 μA; temperature 25°C.

Cyclic voltammetry.—Experiments were carried out with an Inelecsa assembly similar to that previously described. All cyclic voltammograms (CVs) were carried out at a constant temperature of 25°C and the solutions were purged with pure nitrogen for 10 min before the voltammetric runs. The return-to-forward peak current ratio, I_{pa}/I_{pc}, for the reversible first electron transfer (the $Ar\text{-}NO_2/ArNO_2^{\cdot}$- couple) was measured, varying the scan rate from 0.1 V s^{-1} to 10 V s^{-1}.

Electrodes.—A BAS hanging mercury drop electrode (HMDE) with a drop surface of 1.90 mm^2 (CV) and a dropping mercury electrode (DME) (DPP and Tast) were used as working electrodes, and a platinum wire served as the counter electrode. All potentials were measured against an Ag/AgCl (KCl sat.) electrode.

Methods.—The experimental I_{pa}/I_{pc} ratios were calculated ac-

[z] E-mail: lnunezv@ciq.uchile.cl

cording to Nicholson's procedure, using individual CVs.[15] Furthermore, E_λ was selected in order to reduce the influence of the second cathodic peak.

Kinetic reaction orders for the nitro radical anion were quantitatively assessed for first- and second-order coupled reactions according to previously published studies.[16-18]

Electrolytic media.—In protic media, all compounds were dissolved in 30% ethanol and diluted with 0.1 M Britton-Robinson buffer solution to obtain final concentrations varying between 0.05 and 5 mM. For the studies in mixed media the following composition was used: 15 mM aqueous citrate/DMF:60/40, 0.3 M KCl and 0.1 M TBAI at different pH, dissolving all isomers in DMF. Finally, the aprotic media consisted of 0.1 M TBAI in DMF for the polarographic and voltammetric experiments. For ultraviolet-visible (UV-vis) and EPR experiments we prefer 0.1 M tetrabutylammonium hexafluorophosphate (TBAHP) in acetonitrile because this solution does not interfere with the spectra.

pH in mixed media.—pH measurements were corrected according to the following expression[19]: $\mathrm{pH}^* - B = \log U_{\mathrm{H}}^0$ where pH* equals $-\log a_{\mathrm{H}}$ in the mixed solvent, B is the pH meter reading, and the term $\log U_{\mathrm{H}}^0$ is the correction factor for the glass electrode, which was calculated for different mixtures of DMF and aqueous solvent according to a previously reported procedure.[20]

Controlled potential electrolysis.—Controlled potential electrolysis (CPE) was carried out on a platinum coil electrode at a controlled potential of −1000 mV for 2-NA and 4-NA and −940 mV for 3-NA both in mixed media at pH 10.5 and in anhydrous dimethyl sulfoxide (DMSO) containing 0.1 M tetra-*n*-butylammonium perchlorate (TBAP) as supporting electrolyte. Oxygen was removed by pure, dry nitrogen presaturated with solvent. A three-electrode circuit with Ag/AgCl (KCl sat.) electrode as reference and a Pt wire as a counter electrode was used. A Wenking potentiostat potentiostat model POS 88 was employed to electrolyze the nitroanisole isomers. To follow the time course of electrolysis, polarography, CV, ESR, and UV-vis spectroscopy were used.

UV-Vis spectroscopic studies.—In order to obtain further information on the progress of the electrolysis, a UNICAM UV-3 spectrophotometer was used. UV-visible spectra were recorded in the 220-800 nm range at different intervals. Acquisition and data treatment were carried out with Vision 2.11 software. An electrolytic cell of our own construction,[21] based on a 1 cm UV cell with a platinum coil as working electrode, was used for the *in situ* generation of the reduction product. The electrolysis was conducted with constant stirring, which was stopped before each measurement.

EPR measurements.—The nitro radical anions of the nitroanisole isomers were generated *in situ* in the EPR cavity by electrochemical reduction at potentials varying between −940 and −1000 mV on a platinum wire at room temperature. The flat electrolytic cell, Wilmad WG-810 (Wilmad Glass, Route 40 and Oak Road, Buena, NJ 08310, USA), includes a pair of platinum electrodes and an Ag/AgCl (KCl sat.) reference electrode. A 5 mM solution of the nitroanisole in aprotic media was purged with nitrogen for 10 min and then reduced. Immediately its EPR spectrum was recorded in the microwave band X (9.67 GHz) in a Bruker ECS 106 spectrometer. Hyperfine splitting constants were estimated to be accurate within 0.05 G.

Digital simulation.—Simulated CV curves were obtained using software DIGISIM® 3.1 CV simulator for Windows. The software was run using a Gateway 2000 PC. An EC_i mechanism type was considered, *i.e.*, an initial one-electron reaction to form the radical anion followed by an irreversible chemical reaction, according to the two possible mechanisms.

Kinetic constants (considering either the dimerization or disproportionation reaction) were calculated from plots of the kinetic parameter, ω, *vs.* the time constant, τ, at a sweep rate of 1 V s^{-1}. For

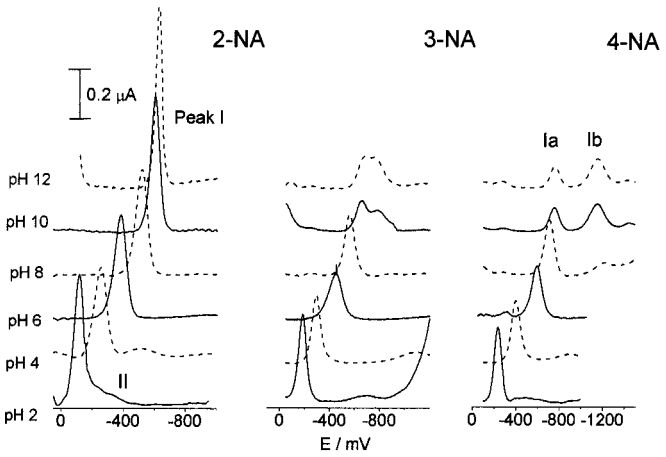

Figure 1. DPP voltammograms of 0.1 mM of each NA isomer in protic medium, 0.1 M Britton-Robinson buffer/ethanol: 70/30 + 0.3 M KCl at different pH.

disproportionation or dimerization we used the theoretical curves described in Ref. 17 or 18, respectively. Finally, a comparison of both experimental and simulated CVs for the different processes was done.

Results and Discussion

Protic media

Polarography.—Each nitroanisole derivative was reduced at the DME in 0.1 M Britton-Robinson buffer/0.3 M KCl/ethanol 70/30. The compounds followed a polarographic behavior with well-defined waves or peaks depending on whether tast polarography or DPP modes were used. In Fig. 1 the differential pulse polarograms for each nitroanisole derivative at different pHs are shown. 2-NA exhibited one well-defined peak (peak I, Fig. 1) over the entire pH range and a second ill-defined one (II) that appeared only at acidic pHs. The peaks are shifted to more cathodic potentials with increasing pH. The 3-NA and 4-NA isomers exhibited the same reduction behavior between pH 2 and 9 (Fig. 1). At pH > 9 the original signal I splits into two new signals (Ia and Ib). In the tast polarographic mode the compounds presented also very well resolved and strongly pH-dependent waves (data not shown). These waves were similar to the peaks found by DPP mode. However, in the case of 3-NA it was not possible to observe a clear separation between waves Ia and Ib in the tast mode.

Figure 2A shows the dependence of peak potential (E_p) with pH for the three isomers. As can be seen from this plot, 2-NA is more easily reduced than the other nitroanisole isomers. Thus, 3-NA and 4-NA were reduced at more cathodic potentials than 2-NA over the entire pH range.

An explanation of this fact is as follows. The −I effect of the $-OCH_3$ group tends to facilitate the $-NO_2$ group reduction just opposite the +M effect that is active at the *ortho* and *para* positions. If the $-NO_2$ group is located in the ortho- or para- position, both opposing effects will be active only if it has some degree of coplanarity with the aromatic ring. The $-NO_2$ group is coplanar with the aromatic system only in the *meta* and *para* positions, but in the *ortho* position it is turned out of the aromatic plane because of steric hindrance with the $-OCH_3$ group. It is therefore more or less affected by the +M effect of the $-OCH_3$ group, depending on the dihedral angle between the $-NO_2$ plane and the plane of the aromatic ring. Solvation of the highly polar $-NO_2$ group is facilitated in protic solvents, thus permitting an increase of the dihedral angle. The shifting of the $-NO_2$ group out of the plane is reflected in the relatively easy reduction of this group in the *ortho* position in a

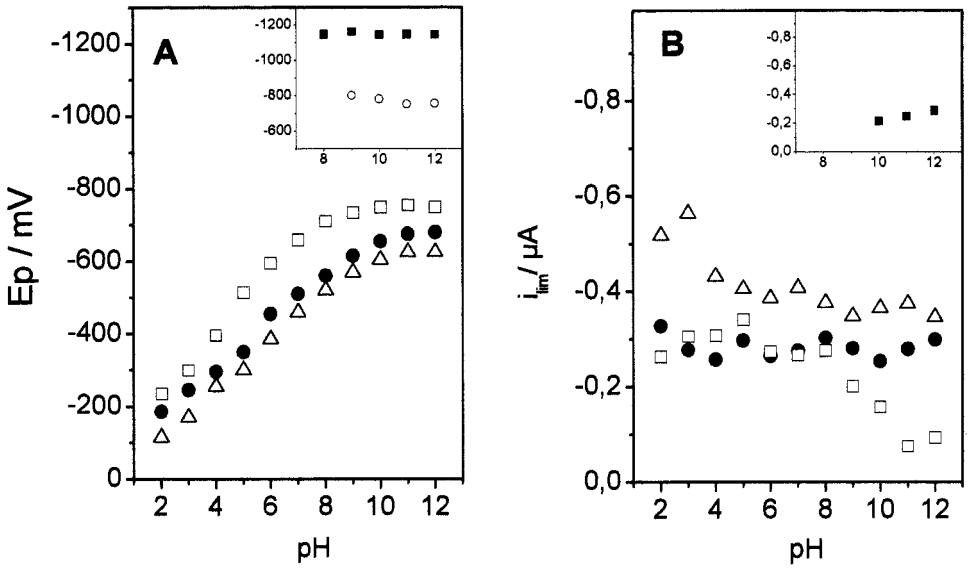

Figure 2. (A) Peak potential and (B) limiting current dependences with pH in protic medium for each NA isomer. Dependence of main signal I and signal Ia: (△) 2-NA, (●) 3-NA, and (□) 4-NA. Inset: dependence of signal Ib for (■) 4-NA and (○) 3-NA.

protic medium. In this case, the loss of coplanarity inhibits the +M effect of the OCH_3 group and the nitro group is mainly affected only by the −I effect of the methoxy group.

Moreover, for 2-NA between pH 2-8 only one linear segment was observed ($\Delta Ep/\Delta pH = -68.4$ mV). At pH > 9, the peak potentials were pH-independent. In contrast, peak I for the 3-NA and 4-NA isomers exhibited two linear segments, with slopes of −54.5 mV/pH (pH 2-5) and −53 mV/pH (pH 6-9) for 3-NA and −80 mV/pH (pH 2-4) and −65 mV/pH (pH 5-9) for 4-NA, and a pH-independent zone past pH 9. The behavior of $E_{1/2}$ of tast polarography with pH was similar to that shown for E_p in Fig. 2A.

When analyzing the behavior of the limiting currents obtained from tast polarograms with pH (Fig. 2B), it is clear that signal I practically remains constant over the whole pH range for 2-NA and 3-NA, indicating its independence on both the kinetics and the reduction mechanism. However, the limiting current for 4-NA presents two pH-independent segments between pH 2-8 and pH 11-12. Between these pH zones,[8-11] a decrease of limiting current was observed concomitant with an increase in the intensity of the new signal Ib (inset Fig. 2B). Doing a ratio between the intensities of waves Ia and Ib at pH 12, we obtained a relationship of 1:3 (Ia:Ib).

A comparison was made of tast polarograms of solutions at the same concentration and pH of each nitroanisole derivative with polarograms of nitrobenzene, which showed that the ratio of their limiting currents was close to 1 between pH 2 and 8, meaning that under these conditions the reduction of the three isomers is due to a four-electron, four-proton reduction, just as for nitrobenzene.[22] Up to pH 8 2-NA adheres to the same mechanism and 4-NA splits this four-electron signal into two new ones with one and three electrons, respectively.

Thus, the polarographic peak (I) corresponds to the reduction of the nitro group to give the corresponding hydroxylamine derivative, according to the well-known overall reaction

$$\text{Ar-NO}_2 + 4e^- + 4H^+ \rightarrow \text{Ar-NHOH} + H_2O \qquad [1]$$

The second peak (II), observed in the acidic range, was strongly pH-dependent and its limiting current value was half that obtained for wave I and can be attributed to a two-electron reduction process of the protonated hydroxylamine to form the corresponding amine derivative, according to the well-known[23,24] reaction

$$\text{Ar-NHOH}_2^+ + 2e^- + H^+ \rightarrow \text{Ar-NH}_2 + H_2O \qquad [2]$$

At alkaline pH (pH > 9), a splitting of the main signal, which is most evident in the 4-NA derivative, indicates the transfer of one electron to the nitro group with the formation of the corresponding nitro radical anion followed by a three-electron transfer to give the hydroxylamine derivative according to the following equations

$$\text{Ar-NO}_2 + e^- \rightleftarrows \text{Ar-NO}_2^{\cdot}\text{-} \qquad [3]$$

$$\text{Ar-NO}_2^- + 3e^- + 4H^+ \rightarrow \text{Ar-NHOH} + H_2O \qquad [4]$$

Cyclic voltammetry.—In the protic medium the nitroanisole isomers gave a well-defined signal (I) that is in accord with the results obtained by polarography (Fig. 3). One main irreversible signal that corresponds to the reduction of the nitro group to the hydroxylamine according to Eq. 1 was observed for 2-NA over the entire pH range and between pH 2 and 8 for 3-NA and 4-NA. At alkaline pH (pH > 7) in the reverse sweep a new signal (III) appears for all the isomers. A 2nd cathodic scan shows a new reduction peak (data not shown), which is paired with the anodic peak III forming a new couple due to the following reaction. This behavior has been previously observed for other nitro compounds[25-27]

$$\text{Ar-NHOH} \rightleftarrows \text{Ar-NO} + 2e^- + 2H^+ \qquad [5]$$

In the case of 2-NA and 4-NA at more cathodic potentials than that of the main signal (I), signal II appeared. This signal corresponds to the reduction of the hydroxylamine involving two electrons to give the corresponding amine, according to Eq. 2.

Studies on the nature of signal I for the three isomers show a linear dependence between $\log I_{pc}$ *vs.* $\log v$ with a slope very close to 0.5, parallel with an independence of $I_{pc}/v^{1/2}$ *vs.* $\log v$. Both results confirm that the reduction of the isomers is diffusion-controlled. Plots between E_p *vs.* log sweep rate at different pH were linear, indicating the irreversibility of the reduction process corresponding to signal I.

Additionally, at pH > 10 a splitting of signal I in two new signals (Ia and Ib) is apparent for both the 3-NA and 4-NA isomers (Fig. 3). However, the electrochemical characterization of such a process was possible only for the 4-NA derivative, where it was clear that signal Ia is reversible and corresponds to the formation of the nitro radical anion.

Characterization of the nitro radical anion from 4-NA in aqueous media.—In Fig. 4, typical CVs of 4-NA in aqueous media are shown. As can be seen from this figure, the isolation of the reversible couple for the nitro radical anion formation was possible at pH 10.5. Thus, the one-electron transfer process appears at $E_{pc} = -755$ mV and $E_{pa} = -810$ mV, with a $\delta E_p \approx 60$ mV, confirming the one-electron transfer process.

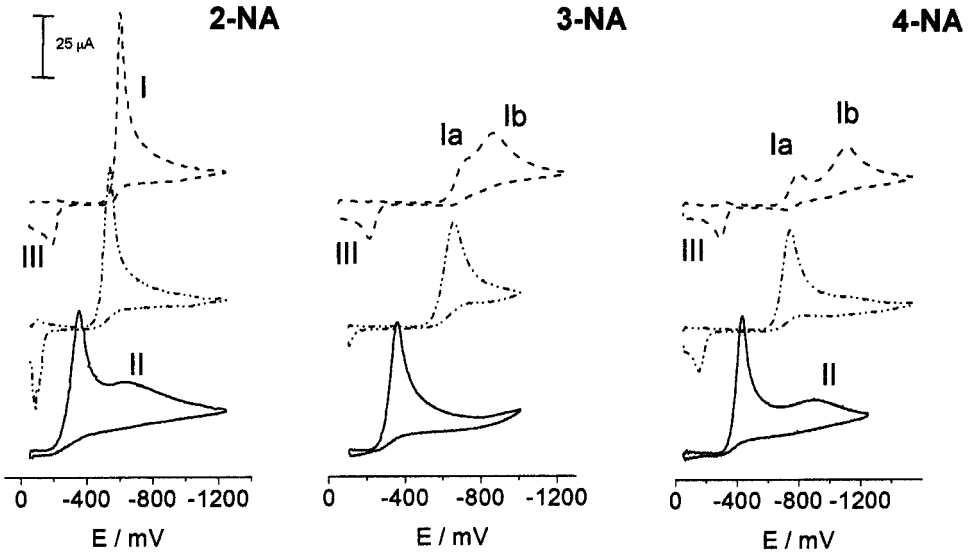

Figure 3. CVs of 1 mM of each NA isomer in protic medium, 0.1 M. Britton-Robinson buffer/ethanol: 70/30 + 0.3 M KCl at (——) pH 3, (—·—·—·—) pH 8, and (— — —) pH 10.5. Sweep rate 1 V/s.

The electrochemical characterization was based on the change in the I_{pa}/I_{pc} ratio,[15] and by applying a well-described methodology the stability of the radical species was studied.[28,29] Results show that as the scan rate increased, the I_{pa}/I_{pc} ratio increased toward unity, typical behavior for an irreversible chemical reaction following a charge-transfer step, *i.e.,* an electrochemical-chemical (EC) process.[15,16] To check the order of the following chemical reaction, the dependence of the I_{pa}/I_{pc} ratio on the concentration of 4-NA derivative was assessed. As predicted by Olmstead[17] for a second-order reaction, the I_{pa}/I_{pc} ratio decreases parallel with the increasing concentration of the electroactive species. This behavior permits us to conclude that the chemical reaction corresponds to the well-known disproportionation of the nitro radical anion, according to

$$2\text{Ar-NO}_2^- + 2\text{H}^+ \rightarrow \text{Ar-NO}_2 + \text{Ar-NO} + \text{H}_2\text{O} \qquad [6]$$

Then the second-order rate constants could be assessed according to Olmstead's procedure[17] using the following relationship

$$\log \omega = \log(k_2 C_0 \tau) \qquad [7]$$

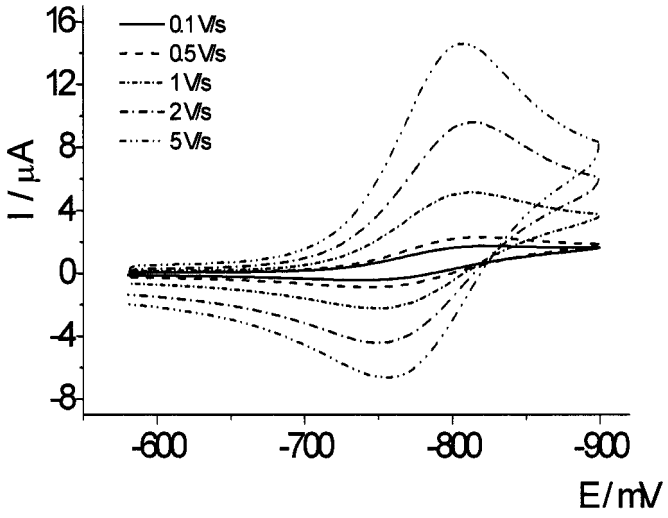

Figure 4. Isolated reversible Ar-NO_2 /Ar-NO_2^- couple for a 1 mM concentration of 4-NA in protic medium, 0.1 M Britton-Robinson buffer/ethanol: 70/30 + 0.3 M KCl at pH 10.5.

Confirming, the second-order character of the following chemical reaction, plots of the kinetic parameter, ω, *vs.* the time constant, τ, at pH 10.5 for 4-NA were linear, with an average correlation coefficient of 0.999.

The second-order rate constant, $k_{2\text{disp}}$, for the nitro radical anion from 4-NA had a value of 19,000 $(\text{M s})^{-1}$ and a half-life, $t_{1/2}$, of 0.05 s for a 1 mM concentration of 4-NA.

Mixed media

Polarography.—Experimental data with these techniques were obtained with the following mixed media: 0.015 M citrate/DMF: 60/40, 0.3 M KCl, and 0.1 M TBAI. Under these experimental conditions, the nitroanisole isomers exhibited by DPP only a single signal (I) between pH 2 and 8, which is shifted to more cathodic potentials with increasing pH. Under these conditions, the single signal corresponds to the reduction illustrated by Eq. 1. However, at pH 9, a splitting of the main signal for all the isomers was observed (Fig. 5). This splitting corresponds to the formation of the nitro radical anion and its subsequent reduction as illustrated by Eq. 3 and 4. Also by the tast polarographic mode, the compounds presented very well resolved and strongly pH-dependent waves (data not shown). These waves were completely equivalent to the peak found by DPP mode.

Figure 6A shows the dependence of the peak potential (E_p) with pH for the three isomers. In this medium, the order of reduction is different from that obtained in protic medium. In DMF/water mixtures 3-NA was more easily reduced than the 2-NA and 4-NA isomers over the entire pH range, and there were no significant differences in reduction potentials between 2-NA and 4-NA. This result is rather different from that obtained in protic media wherein the 2-NA compound was more easily reduced. This difference can be explained as a consequence of solvation effects. In fact, solvation of the highly polar $-NO_2$ group is facilitated in protic solvents, thus permitting the loss of coplanarity between the $-NO_2$ group and the aromatic ring inhibiting the +M effect of the $-OCH_3$ group in the ortho position. When mixed media are used, its protic character is minor compared to that of a completely protic media, and solvation of the highly polar $-NO_2$ group is not facilitated in aprotic solvents, permitting a decrease of the dihedral angle. Consequently, in this case the +M effect of $-OCH_3$ group in the *ortho* position acts to hinder the nitro reduction. Also, it is possible to observe that at pH < 9, the main signal (I) for the 3-NA isomers exhibited two linear segments for the E_p *vs.* pH plots. The E_p/pH dependence can be summarized as follows for the NA isomers: A linear zone at 2 < pH < 6: 2-NA −14 mV/pH, 3-NA −23 mV/pH, and 4-NA −25 mV/pH; a second linear zone at 6 < pH < 9: 2-NA −57 mV/pH,

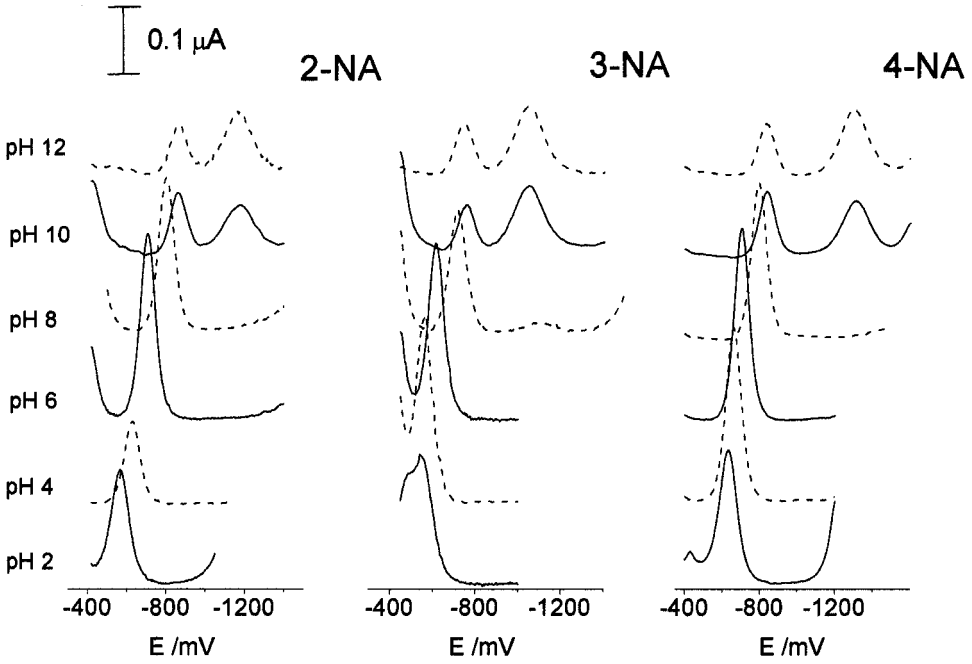

Figure 5. DPP voltammograms of 0.1 mM of each NA isomer in mixed medium, 0.015 M aqueous citrate /DMF: 60/40, 0.3 M KCl and 0.1 M TBAI at different pH.

3-NA −43 mV/pH, and 4-NA −44 mV/pH. At pH > 9, potentials corresponding to signals Ia and Ib (splitting of the main signal) were pH-independent for all the isomers.

Analyzing the limiting current behavior with pH (Fig. 6B), it is clear that between pH 2-8, the limiting currents were pH-independent for signal I for all the isomers in these media. However, beginning at pH 9 the limiting current corresponding to wave I decreased with increasing pH. In contrast, the limiting current corresponding to wave Ib tended to increase with the pH. In this case the relationship Ib:Ia at pH 12 was ~1:2.7.

Cyclic voltammetry.—Our results demonstrated that in acidic and neutral pHs (Fig. 7), nitroanisole isomers were irreversibly reduced according to Eq. 1. However, from pH 8 the main irreversible signal was split into two signals (Ia and Ib) for the three nitroanisoles studied, *i.e.*, a first reversible couple due to the monoelectronic reduction of the nitro group to the corresponding radical anion (according to eq. 4) and at more cathodic potentials, a second irreversible peak corresponding to the three-electron transfer to give the hydroxylamine derivative as shown in Eq. 5. For the kinetic characterization of the radicals in this medium, a similar procedure as described above for the aqueous medium was followed. The results indicated that the mechanism is an EC_i type, since the I_{pa}/I_{pc} ratio increased with increasing sweep rate. Furthermore, a dependence of this ratio on the nitroanisole concentration was observed. In conclusion, the reduction mechanism in the selected mixed media for the three nitroanisole isomers involves two stages: first, a reversible one-electron reduction to form a stable nitro radical anion, followed

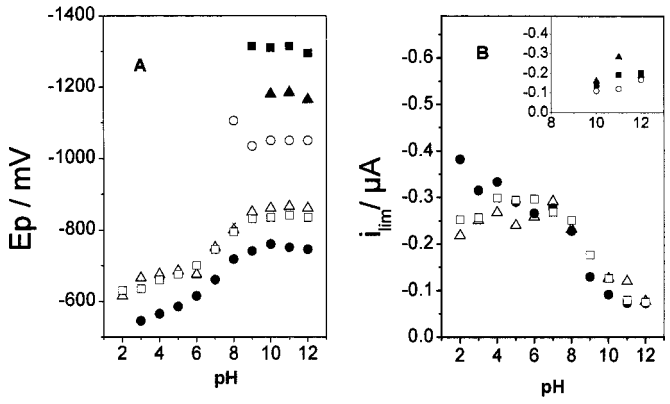

Figure 6. (A) Peak potential and (B) limiting current dependences with pH in mixed medium for each NA derivative. Dependence of main signal I and signal Ia: (△) 2-NA, (●) 3-NA, and (□) 4-NA. Inset: dependence of signal Ib for (▲) 2-NA, (●) 3-NA, and (■) 4-NA.

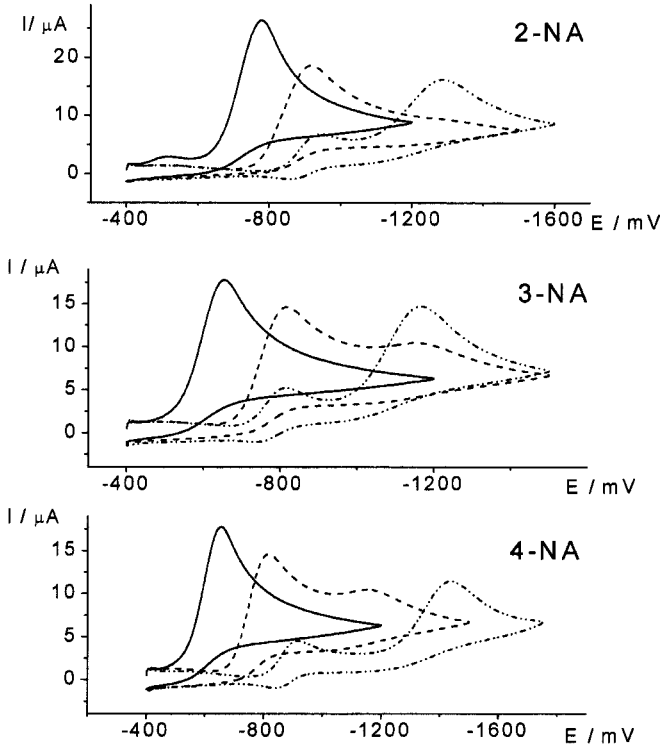

Figure 7. CVs of 1 mM each NA derivative in mixed medium, 0.015 M aqueous citrate/DMF: 60/40, 0.3 M KCl and 0.1 M TBAI at different pHs: () 3, (— — —) 8, (—·—·—·—) 10.5. Sweep rate 1 V/s.

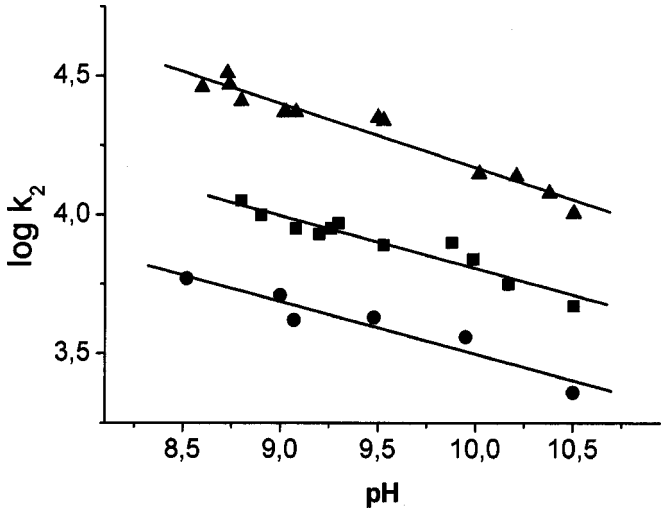

Figure 8. Dependence of calculated k_2 with pH for each NA derivative in mixed medium, 0.015 M aqueous citrate/DMF: 60/40, 0.3 M KCl and 0.1 M TBAL: (▲) 2-NA, (●) 3-NA, and (■) 4-NA.

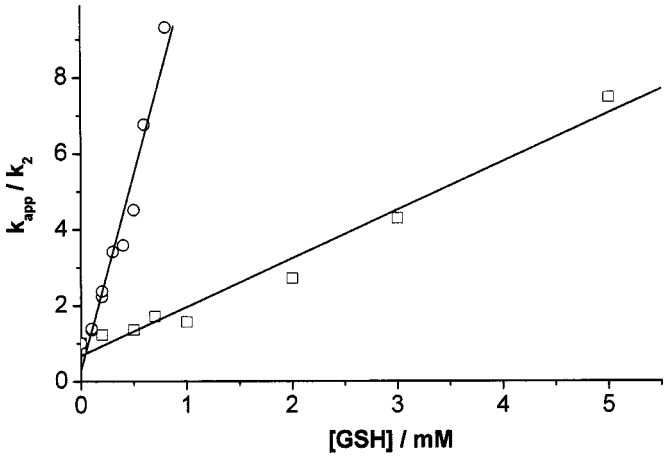

Figure 9. k_{app}/k_2 dependence on GSH concentration for (○) 3-NA and (□) 4-NA.

by a second-order disproportionation reaction of the radical represented by Eq. 6.

This behavior was corroborated for each nitroanisole isomer and at different pH values. Then we calculate the corresponding decay constants. Figure 8 shows the correlation between the calculated k_{2disp} values and the proton concentration. These results clearly demonstrate that when the pH of the reaction medium is increased the stability of the nitro radical anion increases, independent of the position of the nitro group in the molecule. On the other hand, the radical anion electrochemically generated from 2-NA was the least stable species. The proximity of the methoxyl group with respect to the nitro group could explain this result. The methoxy group exerts its donating-electron properties on the latter, making difficult its reduction. For a 1 mM nitroanisole concentration at pH 10.5 the calculated second-order rate constants, k_{2disp}, had an average value of 10,900 ± 930 $(M\ s)^{-1}$, 2400 ± 400 $(M\ s)^{-1}$ and 5000 ± 600 $(M\ s)^{-1}$, for 2-NA, 3-NA, and 4-NA, respectively, for six independent determinations.

Reactivity of the nitro radical anions from nitroanisole isomers toward glutathione.—Cyclic voltammetry proved to be extremely useful for the detection and quantification of the interaction between the one-electron reduction product from the nitroanisole isomers and the endobiotic, glutathione, through modifications in the current-voltage response.

The optimal medium should provide a good stabilization and separation of the nitro radical anion reaction from reactions of other redox intermediates, thus permitting us to study its reactivity with relevant biological targets in isolation. The mixed medium that fulfills these characteristics was: 0.3 M borate buffer/DMF (40/60), 0.015 M aqueous citrate, 0.3 M KCl, and 0.1 M TBAI at pH 9.0. To test the reactivity of the electrochemically generated nitro radical anion with glutathione, a five-step method was applied. First, CVs of glutathione were obtained in the same voltage range and with the same sweep rates in which the nitro radical anion corresponding to the nitroanisole isomers appears. This study showed no peaks for glutathione under the above experimental conditions. Second, the characteristic linear dependence between ω *vs.* τ[17] for a second-order chemical reaction of the radicals was obtained either in the absence (k_{2disp}) or in the presence of the glutathione (k_{app}). However, concomitant with the increase in the concentration of glutathione, an increase in the slopes of the plots was also observed, always keeping correlation coefficients greater than 0.98. This last effect could be explained by the contribution of two different simultaneous competitive decay pathways, *i.e.*, the natural decay of the radical anions and their reaction with glutathione, which can be represented by the following equations

$$2\,\text{Ar-NO}_2^{\cdot}\text{-} + 2\text{H}^+ \xrightarrow{k_{2disp}} \text{Ar-NO}_2 + \text{Ar-NO} + \text{H}_2\text{O} \quad [8]$$

$$\text{Ar-NO}_2^{\cdot}\text{-} + \text{GSH} \xrightarrow{k_{app}} \text{Products} \quad [9]$$

Third, the effect of increasing concentrations of glutathione on the I_{pa}/I_{pc} ratios of the radical at different sweep rates was assessed. Fourth, from the slopes of the plots of ω *vs.* τ in the presence of glutathione, the k_{app} values were calculated. Finally, from plots of $k_{app}/2k_{2disp}$ *vs.* endobiotic concentrations and applying a previously described procedure[28] the interaction rate constants (ki_{app}) were obtained (Fig. 9).

The interaction rate constants (ki_{app}, calculated according to the procedure described in Ref. 28) for the reaction between the nitroanion from nitroanisole and glutathione at pH 9 were 5240 ± 76 $(M\ s)^{-1}$ and 87,000 ± 123 $(M\ s)^{-1}$, for 3-NA and 4-NA, respectively. In the case of 2-NA, a quantitative determination was not possible, but qualitatively a significant reaction could be appreciated. Results from these experiments show that the interaction rate constants (ki_{app}) were higher than the respective rate constant of the natural decay, *i.e.*, 5240 *vs.* 4100 for 3-NA and 87,000 *vs.* 8500 for 4-NA, respectively, at pH 9, indicating that the species markedly reacted with glutathione. In addition to the redox characteristic of the nitro radical anion from the nitroanisoles, prototropic equilibrium controls both the natural decay and its reactivity with glutathione. The protective role of glutathione (GSH) against cytotoxity of nitro radical anions derived from nitroaryl compounds arises from the reaction of $\text{R-NO}_2^{\cdot}$--with R-SH/R-S^-, presumably by the following reaction

$$\text{R-NO}_2^{\cdot}\text{-} + \text{R-S}^- + 2\text{H}^+ \rightarrow \text{R-NO} + \text{R-S}^{\cdot} + \text{H}_2\text{O} \quad [10]$$

Recently[28] we have proved by ESR spectroscopy that under anaerobic conditions the nitro radical anion from nitrofurantoin is scavenged by GSH. Furthermore, to assess the type of interaction between GSH and the nitro radical anion, spin-trapping studies using dimethylnitrosopropane (DMPO) were conducted. After the addition of the spin trap, a typical ESR spectrum of the adduct GS and DMPO appeared. These results substantiate the view that at least partially, the mechanism of the reaction involves the GS species. The present results are in line with these previous studies, indicating that nitro radical anions can be efficiently scavenged by GSH.

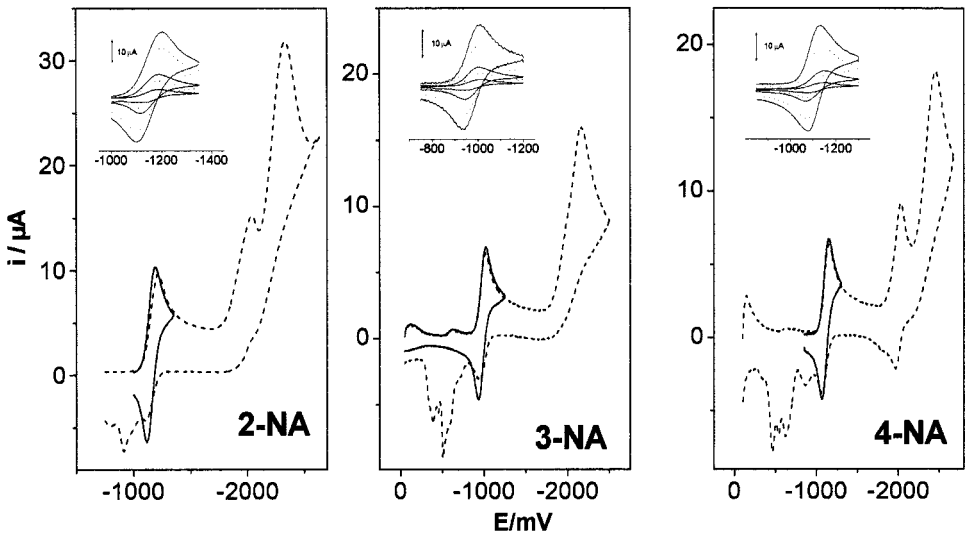

Figure 10. CVs of 1 mM of each NA isomer in aprotic medium, 0.1 M tetrabutylammonium perchlorate in DMF Inset: CVs for each Ar-NO_2 /Ar-$NO_2^{\cdot}$-couple at different sweep rates (0.1, 0.5, 1, 5, and 10 V/s).

Aprotic media

Polarography.—In this medium both in DPP and tast polarography modes the compounds presented two main signals at potentials of $E_p^I = -600$ mV and $E_p^{II} = -900$ mV for 2-NA, $E_p^I = -725$ mV and $E_p^{II} = -1015$ mV for 3-NA, and $E_p^I = -605$ mV and $E_p^{II} = -1000$ mV for 4-NA. The first peak corresponds to the one-electron reduction to give the nitro radical anion and the second peak to the further one-electron reduction to the di-anion.[13,14]

Cyclic voltammetry.—The three isomers exhibited two main signals (Fig. 10), the first one due to the formation of the nitro radical anion involving a one-electron transfer and a second signal appearing at more cathodic potentials, probably due to formation of the di-anion.[13,14] Also, in this medium peak potential values' either anodic or cathodic' were significantly higher than those in mixed media. These last signals were not studied in detail because our main interest was in the first reduction process, *i.e.*, the nitro radical anion formation. The electrochemical characterization of the first reversible couple revealed a similar behavior to that found in mixed media, *i.e.*, an EC_2 process for the three nitroanisole isomers involving two stages. First, a reversible one-electron reduction occurs to form a stable nitro radical anion as in Eq. 3, followed by a reaction of second-order decay of the radical. In the absence of protons, it is more probable that the nitro radical anions decay via dimerization rather than disproportionation. We calculated the decay constant using both approaches, *i.e.*, dimerization and disproportionation.[17,18] In order to check which mechanism fits better we have used a computer simulation. In Fig. 11, the experimental and simulated CVs for the $ArNO_2/ArNO_2^-$ couple at 1 V/s for the 4-NA isomer are shown. From these comparisons it is clear that a dimerization mechanism better simulates the experimental voltammogram. The same results were found at several sweep rates and for the other two nitroanisole isomers (data not shown).

In summary, the nitro radical anion from each nitroanisole isomer in aprotic medium decays via a dimerization reaction, and for a 1 mM nitroanisole isomer concentration, the calculated second-order rate constants, $k_{2\mathrm{dim}}$, had an average value of 1100 $\pm$ 100 $(M\,s)^{-1}$, 1600 $\pm$ 150 $(M\,s)^{-1}$, and 650 $\pm$ 70 $(M\,s)^{-1}$ for 2-NA, 3-NA, and 4-NA, respectively, for six independent determinations. As expected, in aprotic media the nitro radical anion corresponding to 4-NA derivative was the most stable radical species.

Controlled potential electrolysis.—The electrochemical reduction of the nitroanisole isomers to the corresponding nitro radical anions and their detection by EPR were carried out in acetonitrile (ACN). The experimental spectra of these nitro radical anions are shown in Fig. 12 (curves 1A-1C). The interpretation of the EPR spectra by means of a simulation process led us to the determination of the coupling constants for all magnetic nuclei (Table I). The simulated spectra (Fig. 12, curves 2A-2C) show good agreement with the hyperfine assignments, confirming the formation of the nitro radical anions under these electrolytic conditions. There also exists good agreement between our coupling constant values and others previously described for these radicals in the literature.[30] Comparing the E_p values obtained by CV for the nitro radical anion formation with

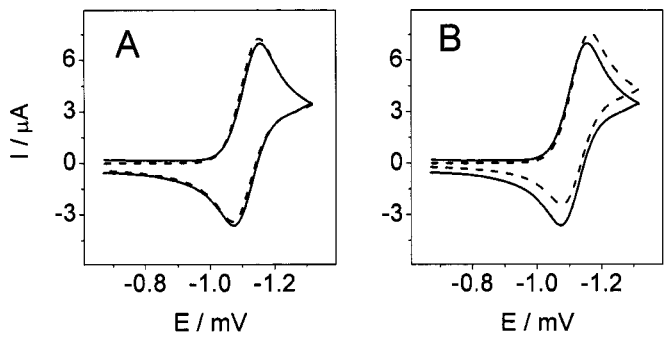

Figure 11. Comparison of (——) experimental and (— — —) simulated CVs from 1 mM 4-NA solutions in an aprotic medium: (A) dimerization and (B) dismutation. Sweep rate 1 V/s.

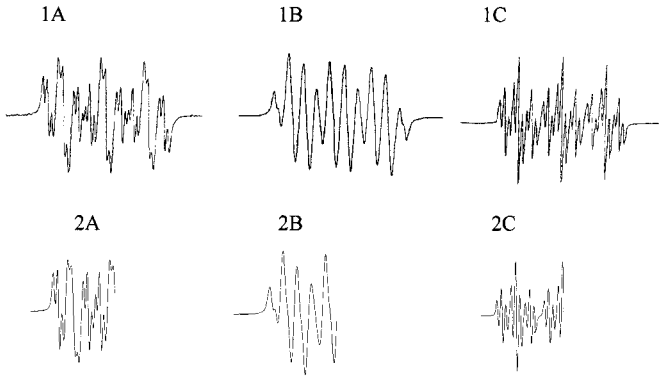

Figure 12. (1) Experimental and (2) simulated EPR spectra of each nitro radical anion electrochemically generated from a 5 mM concentration of (A) 2-NA, (B) 3-NA, and (C) 4-NA.

Table I. Experimental hyperfine coupling constant values for Ar-$NO_2^{\cdot}$- radical anions electrochemically generated from different nitroanisole isomers.[a]

	E_{pc} (mV)	a^N (G)	a^{H2} (G)	a^{H3} (G)	a^{H4} (G)	a^{H5} (G)	a^{H6} (G)
2-NA	−1193	10.52	—	0.91	4.00	1.10	3.54
3-NA	−1027	9.84	2.9	—	3.43	1.14	2.9
4-NA	−1142	11.09	3.32	1.03	—	1.03	3.32
2-NA*		10.56	—	0.90	3.92	1.05	3.55
2-NA*		9.75	3.22	—	3.70	1.0	3.32
4-NA*		11.05	3.36	1.08	—	1.08	3.36

[a] Comparison with values obtained from Ref. 30.

the nitro group nitrogen hyperfine constant (a^N) (Table I), it is possible to observe that there is a correlation. Thus, 3-NA presents the lowest peak potential value concomitantly with the lowest a^N value, such as was described in early reports.[31,32] Then, when a lower spin density resides on the nitro group of the radical anion, the redox potential is less negative.

Applying the same methodology as that in the EPR experiments, UV-vis curves on the time-course of electrolysis for the three isomers were recorded at different intervals in ACN. Figure 12 shows that the original absorptions at $\lambda_{max} = 260$ nm and $\lambda_{max} = 330$ nm corresponding to 2-NA increased during CPE. Moreover, in the inset of Fig. 13 the UV-vis differential spectrum corresponding to a new species electrochemically generated after 40 min electrolysis is displayed. As can be seen, the new species presents a spectrum with maxima at $\lambda_{max} = 289$ nm and $\lambda_{max} = 376$ nm.

In general terms, the other nitroanisole isomers (3-NA and 4-NA) exhibited similar changes, *i.e.*, the differential spectra had the following characteristics: maxima at $\lambda_{max} = 301$ and 365 nm for 3-NA and maxima at $\lambda_{max} = 263$ and 345 nm for 4-NA, respectively.

The results show that significant modifications in UV-vis spectra of nitroanisole isomers after CPE have occurred, which can be summarized as follows: (*i*) increases of absorptivity in the original absorption bands and (*ii*) appearance of new maxima which are obtained from the differential spectra after 30-40 min of electrolysis.

Conclusions

In all the studied electrolytic media, 4-NA was reduced at more cathodic peak potentials and the corresponding radicals were the most stable. Even, kinetic characterization of 4-NA in aqueous medium was possible.

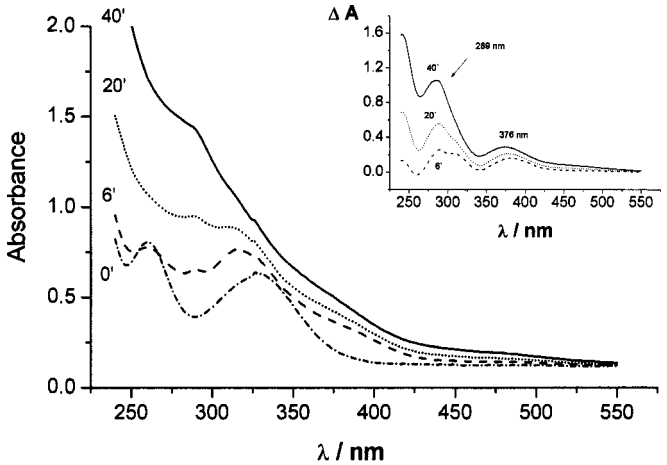

Figure 13. UV is changes of 1 mM 2-NA in aprotic medium at different electrolysis times. Controlled potential −1000 mV in aprotic medium. Inset: Time-course of differential spectra.

The isolation of the reversible couples corresponding to the nitro radical anions in mixed media was achieved at pH ⩾ 10.5. The second-order disproportionation rate constant corresponding to the 2-NA derivative was 4.56 times higher than that of 3-NA [$k_{2disp}^{2\text{-NA}} = 10{,}900\ (M\ s)^{-1}$ *vs.* $k_{2disp}^{3\text{-NA}} = 2400\ (M\ s)^{-1}$].

Nitro radical anions electrochemically generated from the 3-NA and 4-NA isomers significantly reacted with GSH with apparent interaction rate constants (k_{app}) higher than that corresponding to the natural decay (k_{2disp}).

In aprotic media, the nitro radical anions were more stable than in mixed media, with the following dimerization second-order rate constant values: $1100 \pm 100\ (M\ s)^{-1}$, $1600 \pm 150\ (M\ s)^{-1}$, and $650 \pm 70\ (M\ s)^{-1}$ for 2-NA, 3-NA, and 4-NA, respectively.

Acknowledgments

This work was supported by a Grant from FONDECYT, no. 8000016 (Lineas Complementarias). The support of D.I.D. from the University of Chile is also acknowledged.

The university of Chile assisted in meeting the publication costs of this article.

References

1. J. C. Spain, *Annu. Rev. Microbiol.*, **49**, 523 (1995).
2. C. Vorbeck, H. Lenke, P. Fischer, J. C. Spain, and H. J. Knackmuss, *Appl. Environ. Microbiol.*, **64**, 246 (1998).
3. L. Sjoberg and T. E. Eriksen, *J. Chem. Soc., Faraday Trans. 1*, **76**, 1402 (1980).
4. C. Corvaja, G. Farnia, and E. Vianello, *Electrochim. Acta*, **11**, 919 (1966).
5. Ya. Stradyn, R. Gavar, L. Baumane, B. Vigante, and G. Dubur, *Chem. Heterocyclic Comp.*, **33**, 184 (1997).
6. E. Constantinescu, M. Hillebrand, and E. Volanski, *J. Electroanal. Chem.*, **256**, 95 (1988).
7. L. Baumane, L. J. Stradins, R. Gavars, and G. Duburs, *Electrochim. Acta*, **37**, 2599 (1992).
8. J. Y. David, J. P. Hurvois, A. Tallec, and L. Toupet, *Tetrahedron*, **51**, 3181 (1995).
9. L. J. Núñez-Vergara, S. Bollo, C. Olea-Azar, P. A. Navarrete-Encina, and J. A. Squella, *J. Electroanal. Chem.*, **436**, 227 (1997).
10. M. M. Ellaithy and P. Zuman, *J. Pharm. Sci.*, **81**, 191 (1992).
11. M. Stiborova, H. H. Schmeiser, and E. Frei, *Collect. Czech. Chem. Commun.*, **63**, 857 (1998).
12. J. G. Hengstler, J. Fuchs, U. Bolm-Audorff, S. Meyer, and F. Oesch, *Scand. J. Work Environ. Health*, **21**, 36 (1995).
13. G. Farnia, G. Megoli, and E. Vianello, *J. Electroanal. Chem.*, **50**, 73 (1974).
14. G. Farnia, A. Roque Da Silva, and E. Vianello, *J. Electroanal. Chem.*, **57**, 191 (1974).
15. R. S. Nicholson, *Anal. Chem.*, **38**, 1406 (1966).
16. G. Bontempelli, F. Magno, G. Mozzochin, and R. Seeber, *Ann. Chim. (Rome)*, **79**, 103 (1989).
17. M. Olmstead and R. S. Nicholson, *Anal. Chem.*, **41**, 862 (1969).
18. M. Olmstead, R. Hamilton, and R. S. Nicholson, *Anal. Chem.*, **41**, 260 (1969).
19. A. G. Gonzalez, F. Pablos, and A. Asuero, *Talanta*, **39**, 91 (1992).
20. A. G. Asuero, M. A. Herrador, and A. G. González, *Talanta*, **40**, 479 (1993).
21. L. J. Núñez-Vergara, J. C. Sturm, A. Alvarez-Lueje, C. Olea-Azar, C. Sunkel, and J. A. Squella, *J. Electrochem. Soc.*, **146**, 1478 (1999).
22. P. Zuman and Z. Fijalek, *J. Electroanal. Chem.*, **296**, 583 (1990).
23. J. Grimshaw, in *Electrochemical Reactions and Mechanisms in Organic Chemistry*, Chap. 11, p. 376, Elsevier, New York (2000).
24. J. C. Sturm, L. J. Núñez-Vergara, J. de la Fuente, C. Castro, P. Naverrete-Encina, and J. A. Squella, *J. Electrochem. Soc.*, **148**, 1 (2001).
25. S. Bollo, L. J. Núñez-Vergara, J. Carbajo, and J. A. Squella, *J. Electrochem. Soc.*, **147**, 3406 (2000).

26. S. Bollo, L. J. Núñez-Vergara, and J. A. Squella, *Bol. Soc. Chi. Quim.*, **44**, 67 (1999).
27. A. El Jammal, J. C. Vire, G. J. Patriarche, and O. Nieto-Palmeiro, *Electroanalysis*, **4**, 57 (1992).
28. L. J. Núñez-Vergara, F. García, M. M. Domínguez, J. De la Fuente, and J. A. Squella, *J. Electroanal. Chem.*, **381**, 215 (1995).
29. L. J. Núñez-Vergara, J. C. Sturm, C. Olea-Azar, P. Navarrete-Encina, S. Bollo, and J. A. Squella, *Free Radical Res.*, **32**, 399 (2000).
30. Lanbolt-Börnstein, *Numerical Data and Functional Relationships in Science and Technology*, H. Fischer and K. H. Hellwege, Editors, Part d1, Vol. 9, p. 499, 500, Springer-Verlag, New York (1980).
31. D. Meisel and P. Neta, *J. Am. Chem. Soc.*, **97**, 5198 (1975).
32. P. Neta, M. G. Simic, and M. Z. Hoffman, *J. Phys. Chem.*, **80**, 2018 (1976).